frontiers | Frontiers in Earth Science

TYPE Original Research
PUBLISHED 10 January 2023
DOI 10.3389/feart.2022.1123747

OPEN ACCESS

EDITED BY
Honglei Wang,
Nanjing University of Information Science and Technology, China

REVIEWED BY
Chao You,
Nanjing University of Aeronautics and Astronautics, China
Chao Wang,
Civil Aviation Flight University of China, China

*CORRESPONDENCE
Ning Yang,
yangn@czust.edu.cn

SPECIALTY SECTION
This article was submitted to Atmospheric Science, a section of the journal Frontiers in Earth Science

RECEIVED 14 December 2022
ACCEPTED 29 December 2022
PUBLISHED 10 January 2023

CITATION
Yang N, Jiang W, Jin C, Zhang S and Hou W (2023), Numerical simulation of the effect of atmospheric condition on the lightning strike for wind turbine.
Front. Earth Sci. 10:1123747.
doi: 10.3389/feart.2022.1123747

Numerical simulation of the effect of atmospheric condition on the lightning strike for wind turbine

Ning Yang[1]*, Wei Jiang[1], Chenlu Jin[2], Shuqin Zhang[1] and Wenhao Hou[3]

[1]Changzhou Institute of Technology, Changzhou, China, [2]Nanjing Meteorological Bureau, Nanjing, China, [3]Jiangsu Provincial Meteorological Bureau, Nanjing, China

The risk of lightning exposure increases as wind turbine size increases, and lightning accidents have grown up to be a severe threat to wind turbines. The present paper focuses on the influence of the changes in atmospheric conditions around the rotating blade for the upward leader initiation. A 2D computational fluid dynamics model was established to obtain the air pressure distribution around the blades, and the simplified inception model was used to determine the initiation of the upward leader mechanism. In this paper, two significant factors of velocity and attack angle were studied. The results show that the trigger height is about an 11.2% difference for 120 m/s with the peak current of return stroke at 30 kA; the difference has reached about 28% for the attack angle of 10°. The research indicates that the area with higher air pressure is exposed to a greater risk of lightning strikes, and the probability of lightning strikes will increase as the blade attack angle increases.

KEYWORDS

lightning strike, wind turbine, air pressure distribution, upward leader inception, positive streamer

Introduction

In recent years, wind energy has grown to be a significant source of sustainable energy to reach emission reduction. Wind turbine installation capacity has increased rapidly in order to meet carbon peak and neutrality targets, which have become common sustainability goals around the world. Based on GWEC (Global Wind Energy Council. 2022) reports, the global wind power total installed capacity reached 837 GW by the end of 2021, about 12.4% growth compared to 2020. With the progress of material technology (such as carbon and glass fiber-reinforced polymers), wind turbine blades have experienced an enormous development due to the new material. Therefore, the size of wind turbines has tremendously increased in recent decades. A large percentage of wind turbines are likely to be installed in places with significant lightning activity [SArajcev et al., 2013]. Lightning strikes on wind turbines are strongly influenced by topological factors, wind turbines installed in mountainous areas are riskier to lightning damage than wind turbines installed in coastal regions [McNiff et al., 2002]. Thus, it is expected that wind turbines need to suffer greater lightning strikes (Agoris, 2002; Cotton et al., 2001; Sorensen, 1998).

Lightning is a tremendous nature phenomenon, the number of lightning strikes increases with structure height, posing significant challenges to wind turbines of growing size (Beckers, 2016). The threat posed by lightning strikes has increased, and caused significant damage due to both direct and indirect effects. According to the insurance company report, lightning strikes cause 23.4% of wind turbine failures in the United States (Gcube-insurance, 2012). Damages to the wind turbine occurred to the blades, rotor, and generator. The blades are the key

components that convert wind energy to mechanical energy, and it is also one of the wind turbine's most vulnerable parts. According to a report from the ECN (Energy Research Centre of the Netherlands), the blades have the highest frequency of lightning strikes (approximately 75%), as well as the most extended downtime (about 10 days per lightning incident) (Rademakers et al., 2002). About 118 lightning strike accidents were recorded, the research has shown that 88.1% were attached to the blade tips. (Madsen et al., 2006). Garolera analyzed 304 cases of lightning-striking accidents in the USA and noted that most of the lightning strike is located at the blade tip, with about 90% of incidents located at the last 4 m of the blade (Garolera et al., 2014). Furthermore, 739 lightning incidents were observed during 7 years, but more than 1032 failures were found. That were indicating a single lightning strike can cause multiple component damage (Rademakers et al., 2002). Despite the fact that wind turbine being equipped with lightning protection equipment, lightning strikes have occurred nevertheless. This is because the manufacturers' design lightning protection devices mainly regard lightning strikes occurring at the place of the maximum electric field strength, for wind turbines that are the tip of blades. Remarkably, the lightning statistics data for wind turbines shows that only about 60% of lightning strikes occur at the blade tip (maximum electric field strength). However, there are still close to half of the lightning strikes occurring outside the vulnerable lightning strike area. The considerable number of existing protection failures indicates this direction is worth further study.

Different researchers have conducted some experiments with the scaled models to investigate the lightning characteristics. Radicevic presented a study with the reduced-size model, and the result shows the rotation of the blades decreases the number of direct lightning strikes. (Radicevic et al., 2012). Wen experimented with a scaled model and switching impulses (250/2500 μs), and the result indicates that the rotation of the blades improves lightning triggering ability (Wen et al., 2016). Furthermore, A comparison between current parameters from stationary and rotating wind turbines was carried out, and it reveals there is no substantial difference between the two operational modes (Yu et al., 2022). From the above study, some ambiguous and even conflicting conclusions have been obtained, and these results are confusing.

The blades of wind turbine generate periodic electric discharges indicating that the effect of rotation plays a critical role [Montanya et al., 2013]. Meanwhile, the lightning development and attachment mechanism considering space charge density distribution were carried out by some researchers. Gu discovered the electric field distortion produced by the space charge and discussed the variation of the streamer during the discharge process [Gu et al., 2020]. To determine the mechanisms of corona and leader initiation for rotating wind turbines, Yu established a three-dimensional drift and diffusion model. The results reveal that as the spinning speed increases, it becomes more sensitive to initiating corona discharge (Yu et al., 2017). Qu proposed a model to investigate the distribution of charged particle migration. It was further discovered that the rotation effect reduces positive ion concentration (Qu et al., 2019). Wang conducted long-gap discharge experiments to determine the difference in lightning triggering ability between rotating and stationary blades. According to the study, rotation increases its capacity to generate lightning strikes [Wang et al., 2017]. However, the space charge distribution is not the only factor that can influence the upward leader initiation when the blades are rotating. These studies have been limited to the shielding effect of space charges generated by thundercloud electric fields. The effect of the change of atmospheric conditions around the blades due to the rotation is neglected. Nevertheless, this factor is strong enough to influence the initiation process of the upward leader. But very few existing studies have paid attention to this point. M. Ramirez carried out a research to investigate the impact of air density on the discharge process [M. Ramirez et al., 1990]. The influence of pressure and humidity on the corona onset performance was studied, and a mathematical model to evaluate the corona onset voltages was proposed (Hu et al., 2011). Yu examined the corona discharge at low atmospheric pressure and discovered that the corona inception voltage drops as atmospheric pressure falls. (Yu et al., 2006). However, the above studies are concentrated on static conditions, and no further research has been proposed for dynamic systems. Therefore, it is necessary to conduct a numerical simulation to analyze the lightning strike characteristics for rotating blades considering the atmospheric conditions. In this paper, a 2D numerical model of air pressure distribution was established. Combining the inception model of upward leaders, the relevant sensitive factors were examined. Furthermore, the vulnerable strike areas of the blade were analyzed. The study will give a theoretical foundation for wind turbine lightning strike performance.

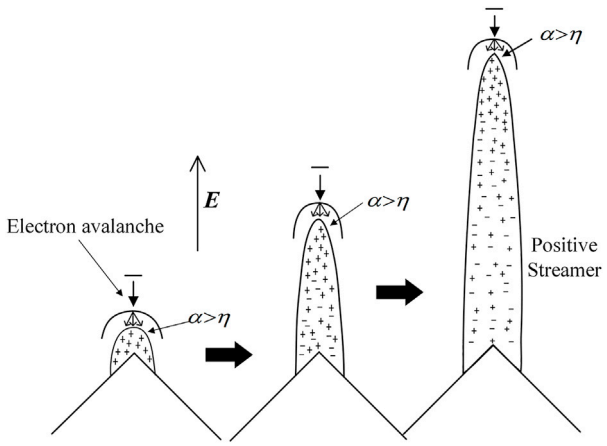

FIGURE 1
Formation of a positive streamer in the enhanced electric field.

Methods

In the second or subsequent streamer bursts, the streamer-leader transform condition is equal to or greater than approximately 1 μC (Gallimberti, 1979; Lalande et al., 2002). Once the requirement is reached, the ionization process provides the energy and current to sustain the thermal transition. At the same time, the upward leader channel expansion generates the electric field to enable the ionization process (Goelian et al., 1997). If this process reaches a dynamic equilibrium, the upward leader–streamer system can develop continuously and steadily.

According to the streamer criterion, free electrons are accelerated under electric field E. The impact ionization of neutral gas particles

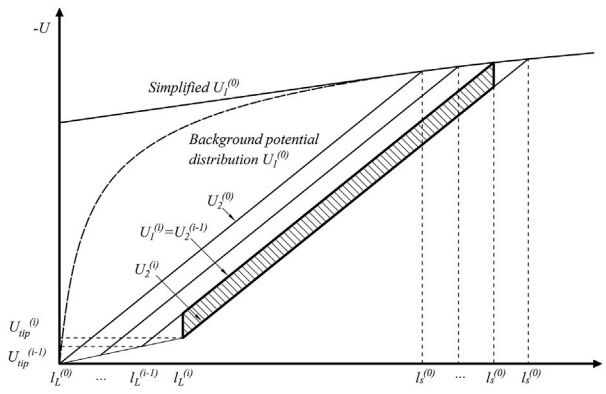

FIGURE 2
The background potential distribution.

increases the electrons. A net ionization coefficient α' can be defined as:

$$\alpha' = \alpha(E) - \eta(E) \tag{1}$$

Where $\alpha(E)$ and $\eta(E)$ are functions of E representing ionization and attachment coefficient, respectively. Defining the distance between $\alpha(E)$ and $\eta(E)$ where they are equal (α' =0) is l. The criterion from the conversion of electron avalanche to streamer is given below:

$$\int_0^l (\alpha(E) - \eta(E))dl \geq \ln\ (N_{stab}) \tag{2}$$

Where, N_{stab} is the critical number of positive ions, taken as 55×10^8 γ is the absolute humidity, P_w is the partial pressure of water vapor, α_w and α_d are ionization coefficients in water vapor and dry air, η_w and η_d are attachment coefficients.

Eq. 1 is only valid for $\alpha' > 0$. The electronic avalanche process is formed with the number of electrons increasing exponentially. The electric field gets greater ahead of the space charge zone, resulting in more positive space charges enter to the electrode gap to neutralize the positive space charges, as shown in Figure 1. When the stability number of positive ions or electrons at the head of the avalanche exceeds N_{stab}, the streamer is assumed to be formed. The average electric field of the streamers E_{str} is affected by the air humidity and the relative air density according to (Eriksson et al., 1986)

$$E_{str} = 425\delta^{1.5} + (4 + 5\delta)\gamma \tag{3}$$

$$P(z) = P_0 \exp\ (-z/z_0) \tag{4}$$

$$T = T_0 - 6H_L \tag{5}$$

$$\gamma = \gamma_0 \exp\ (-H_L/z_H) \tag{6}$$

Where γ is the absolute humidity, δ is the relative air density given by $\delta = (P/P_0)(T_0/T)$, in which P is the atmospheric pressure, T is the temperature, P_0 is the standard atmospheric pressure (1013.25 hPa), H_L is the altitude (km), and T_0 is 293 K; E_{str} is equal to 52 MV/m under the standard atmospheric condition (P=P_0, T=T_0; $\gamma = 11 g/m^3$). It is worth noting that it can be considered as a constant value for stationary objects, but it is necessary to make the corrections for a dynamic system.

In order to determine the stable upward leader's inception, the positive upward-leader inception theory is adopted (Becerra and Cooray, 2006a; Becerra and Cooray, 2006b). The method of approximate geometric based on the background potential distribution was presented. When △Q is greater than 1 μC, it is considered that the unstable upward leader has been generated since the background potential is strong enough to create a second corona charge. Furthermore, if the leader length exceeds the maximum value of 2 m, the steady leader inception criterion is considered satisfied. Otherwise, the development of the upward leader is considered to be terminated.

Charge conservation theory states that the quantity of charge entering the leader should be equal to the number of space charges remaining in the corona zone. The background potential distribution $U_1^{(0)}$ shift to $U_2^{(0)}$ for the reason of space charge existence and expressed as a straight line, the slope is E_1 and the intercept of the vertical axis Is $U_0^{'}$, as Figure 2 shows. Accordingly, the distribution of background potential can represented as:

$$U_1^{(0)} \approx E_1 \cdot l + U_0^{'} \tag{7}$$

According to the approximate geometric method, the second corona charge defines as:

$$\Delta Q^{(0)} \approx K_Q \cdot \frac{l_s^2}{2} \cdot (E_{str} - E_1) \tag{8}$$

When thermal ionization is completed (temperature above 1500 K), the stem is transited to the leader with increased conductivity and energy as $\Delta Q^{(0)} \geq 1\,\mu C$. The potential for the tip of leader can be computed with:

$$U_{tip}^{(i)} = l_L^{(i)} \cdot E_\infty + x_0 \cdot E_\infty \cdot ln\left[\frac{E_{str}}{E_\infty} - \frac{E_{str} - E_\infty}{E_\infty} \cdot e^{-l_L^{(i)}/x_0}\right] \tag{9}$$

The charge ΔQ can be calculated as:

$$\Delta Q \approx K_Q\left[\left(E_{str} \cdot \left(l_L^{(i)} - l_l^{(i-1)}\right) + U_{tip}^{(i-1)} - U_{tip}^{(i)}\right) \cdot \left(l_s^{(i-1)} - l_L^{(i)}\right)\right] \tag{10}$$

The developed distance of the upward leader and the corona can be expressed with:

$$l_s^{(i)} = l_s^{(0)} + \frac{E_{str} \cdot l_L^{(i)} - U_{tip}^{(i)}}{E_{str} - E_1} \tag{11}$$

$$l_L^{(i+1)} = l_L^{(i)} + \Delta l_L^{(i)} = l_L^{(i)} + \frac{\Delta Q}{q_L} \tag{12}$$

When l_L reaches 2 m, the stable upward leader requirement is satisfied. Once $\Delta l_L^{(i)} < 0$, the development of the upward leader is terminated. The relevant parameters are shown in Table 1. In a previous study, the validity of model was examined by comparing simulated results with optically observed data which shows great agreement. (Yang et al., 2017).

The positive streamer gradient is affected by the atmospheric conditions (air humidity and air pressure), which make significant changes to lightning strike performance. Hence, it can obtain a method to determine the initiation of the upward leader by taking the atmospheric condition as an essential factor from the above correlating formulas. It is important to note that the lightning strike is assumed to be taken place successfully when the inception condition of the upward leader is satisfied in this study. The initial point is considered the subsequent strike point.

Results

The geometry of the wind turbine increases with the installed capacity, and the blade length also increases accordingly, which leads

TABLE 1 The parameters.

Parameter	Description	Value	Units
$I_L^{(1)}$	Initial leader length	5×10^{-2}	m
E_{str}	Positive streamer gradient	4.5×10^{5}	V/m
E_{∞}	Final quasi-stationary leader gradient	3×10^{4}	V/m
x_0	Constant given by the ascending positive leader speed and the leader time constant	.75	m
q_L	Charger per unit length necessary for thermal transition	6.5×10^{-7}	C/m
K_Q	Geometrical constant	4×10^{-11}	C/Vm

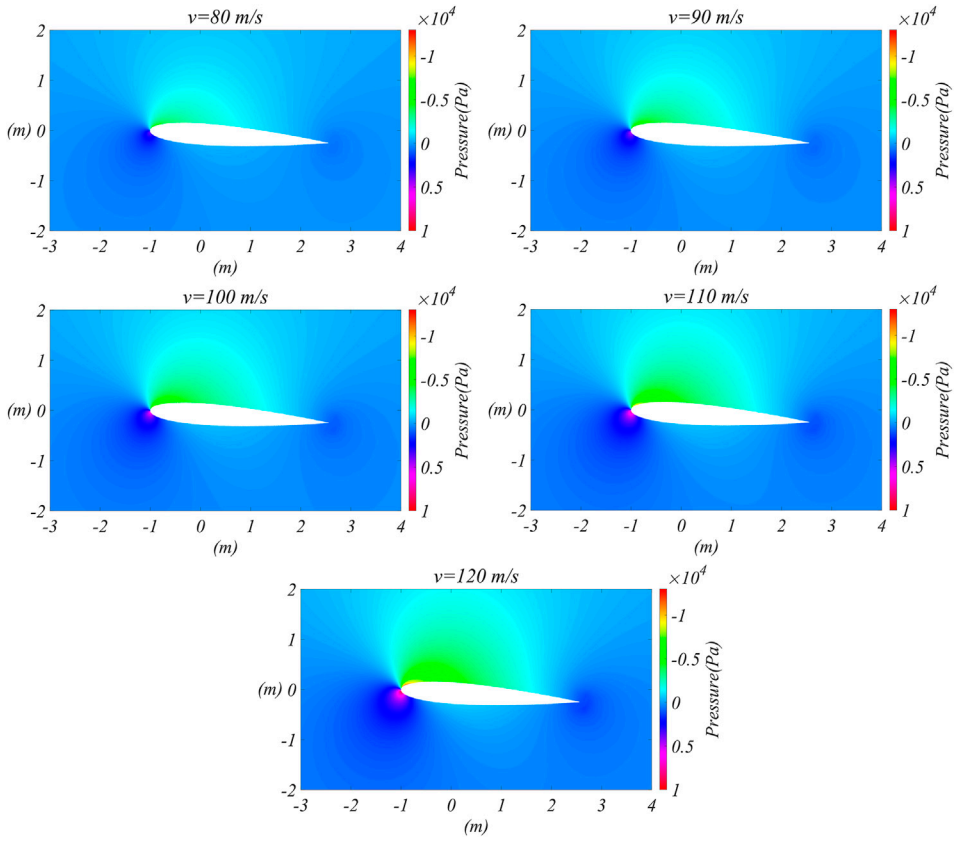

FIGURE 3
The air pressure distribution at different velocities around wind turbine blade.

to the blade tip speed becoming higher. As a result, precisely predicting a lightning strike to a wind turbine is critical. The study applies the geometry of a 2 MW wind turbine model with a 95 m hub and 54 m blades, with rotational speeds ranging from 8.1 rpm to 19 rpm according to the wind. The linear velocity of the blade tip is between 45 and 110 m/s. It is faster than wind speed, but much slower than the downward stepped leader (approximately 10^5–10^6 m/s). For the sake of a quantitative study, a symmetric wing NACA0012 was used in this research. Different speeds and attack angles were used as variables in this study to discuss the lightning strike characteristics of wind turbines under different conditions.

According to Bernoulli's theory, the air velocity on the top surface of the airfoil is greater than on the bottom. Hence, the atmospheric pressure on the blade surface is unequal (the pressure on the lower surface is high and the upper surface is low), and it depends on the two factors of velocity and attack angle. To analyze the lightning striking characteristics of the wind turbine, the air pressure distribution around the blade must be obtained. In this paper, a commercial finite element method (FEM) program based on the COMSOL software (Comsol Group, 2014) is used to analyze the pressure distribution. A two-dimensional model is made for the sake of achieving a balance between computational speed and accuracy.

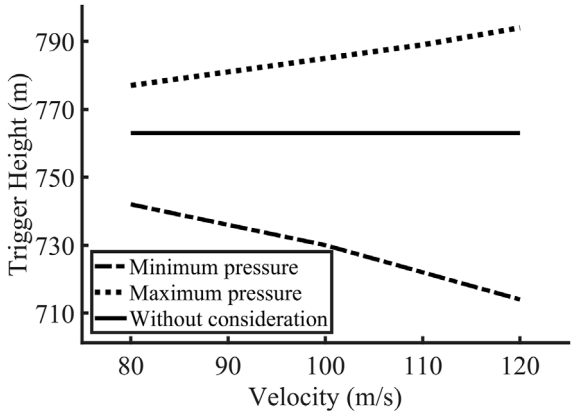

FIGURE 4
The trigger height at different velocities for minimum and maximum air pressure area.

From the above, it is known that the inception of the upward leader is a necessary condition for the object to be struck by lightning. The major factors must be identified to investigate the upward leader development process. Firstly, the effect of the velocity of the blade is considered. Figure 3 shows the simulated result of air pressure distribution for several different velocities of the blade, the attack angle is set to 4°. As can be seen, the difference in air pressure increases while the blade speeds up. Several velocities between 80 m/s to 120 m/s are simulated, respectively. The simulation result shows that the minimum pressure (relative pressure) is close to -1.22×10^4 Pa when the blade speed is at 120 m/s, while the maximum pressure (relative pressure) reaches 8.93×10^3 Pa. Therefore, the difference of pressure could cause a huge change in the positive streamer gradient, which can lead to a considerable change in lightning strike characteristics according to Eq. (3). Based on the simulation results, the positive streamer gradient varies between 4.43×10^5 V/m and 5.87×10^5 V/m in this case.

This study makes the assumption that the downward stepped leader channel is vertical with branch-free and non-uniform charge density distribution, which can be expressed as a function of the return stroke peak current (Cooray et al., 2007). In this case study, the return stroke peak current is taken as a typical value with 30 kA. As the downward-stepped leader moves toward the ground, an upward leader can be initiated when downward-stepped leader descends to a certain height. There is a decreasing trend with the increasing velocity at minimum pressure area, which equals 742 m at the velocity of 80 m/s, while it is approximately 714 m for the

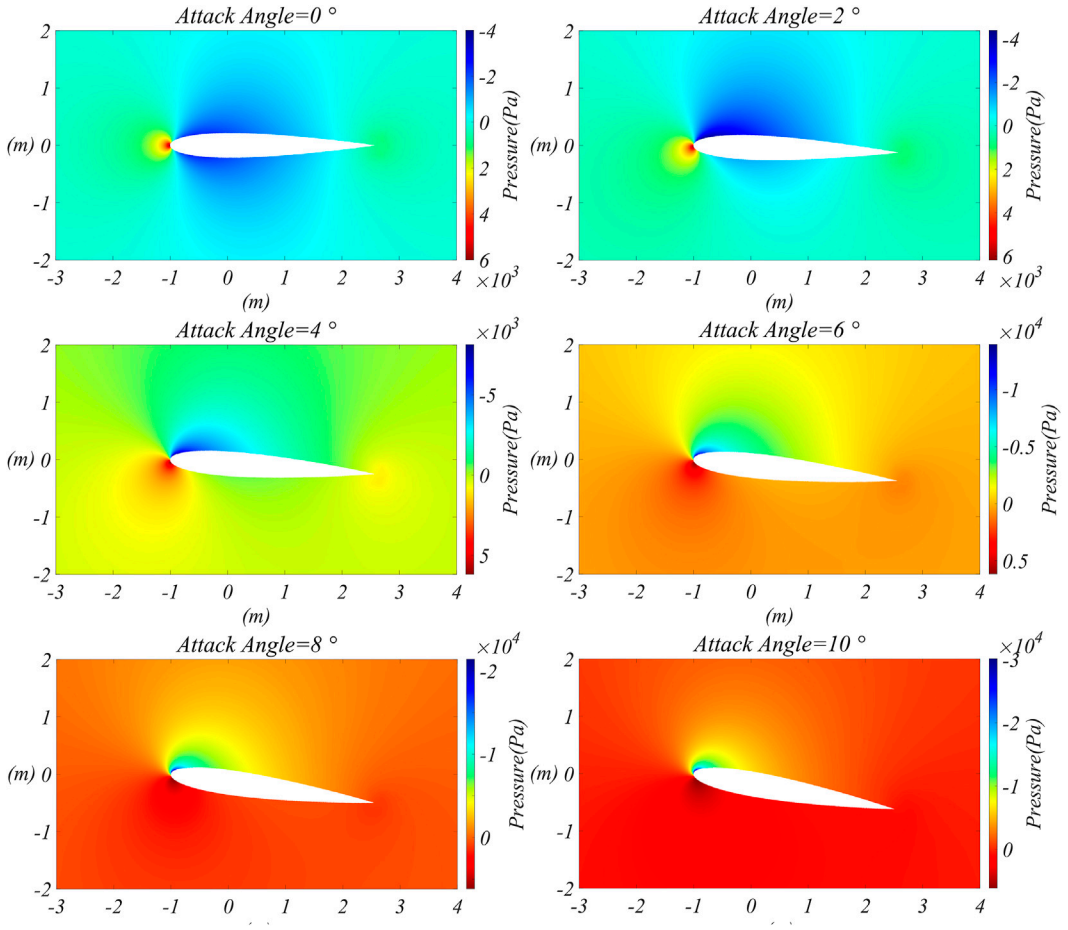

FIGURE 5
The air pressure distribution for different attack angles around wind turbine blade.

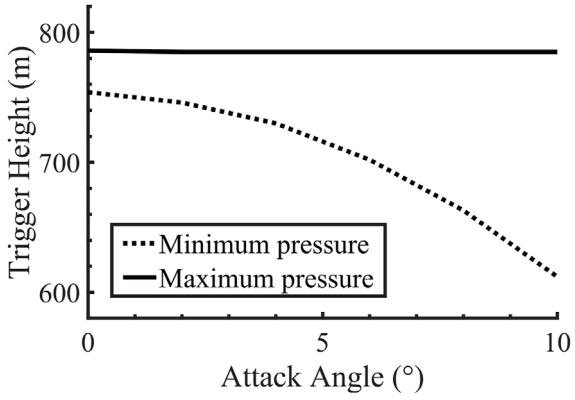

FIGURE 6
The trigger height of different attack angles for minimum and maximum air pressure area.

velocity at 120 m/s. However, the maximum pressure area shows the opposite trend. Note that if the effect of air pressure change is not considered, the downward-stepped leader trigger height is a fixed value of 763 m regardless of how fast the blade rotates. From the above results, it can be seen that the region where the air pressure is higher will be more likely to trigger a lightning strike than the lower-pressure region. The trigger height for the two different regions reaches 714 m and 794 m at 120 m/s, respectively. There is about an 11.2% difference between the two regions, as shown in Figure 4.

On the other hand, the attack angle is also regarded as an important factor. A similar method is adopted, the simulation result of pressure distribution for different attack angles is obtained, represented in Figure 5. In this case study, the obtained result is simulated with different attack angles from 0 to 10° at 100 m/s (the airflow separation effect occurs as the angle of attack increases, there are no more discussion for larger attack angles), respectively. The change in the pressure result in a considerable variation of the positive streamer gradient, which varies between 3.19×10^5 V/m and 5.67×10^5 V/m in this case. The trigger height that makes the upward leader successfully initiated was correspondingly changed. The simulation results are depicted in Figure 6. It is shown that the trigger height decreases dramatically with increased attack angle for the low-pressure area (0°–10°). But this trend in the high-pressure area is not significant. The trigger height is 785 m for the high-pressure area, and is reduced to 612 m in the low-pressure area (−28% reduction) for the case of 10°. The difference in trigger height tends to increase gradually with the increase of the attack angle. According to the simulated results, it can be concluded that the probability of lightning strikes in the low-pressure area will be reduced as the attack angle increases for the blade.

Conclusion and discussion

According to the statistics, lightning strikes have already become a severe threat to wind turbines that could cause enormous damage. The size of the wind turbine is getting increasingly larger, which faces more potential threats. As a result, it is expected that the wind turbines would be suffered more lightning strikes. In this paper, a 2D computational fluid dynamics model was established to obtain the distribution of the air pressure field around the blade. Aside from that, an upward leader inception model was established as well, and the initiation process of the upward leader on the blade for different velocities and attack angles was calculated. It can be found that there is a severe shortage without considering the changes in air pressure. The related conclusions are given as follows.

1 The difference between the maximum and minimum air pressure values increases as the blade accelerates, which can reach 2.11×10^4 Pa at 120 m/s. The changes result in the positive streamer gradient varying between 4.43×10^5 V/m and 5.87×10^5 V/m, which leads to a considerable difference in the lightning strike characteristics for the wind turbines.
2 The trigger height decreases with the increasing velocity at the minimum pressure area. However, the maximum pressure area shows the opposite trend. The trigger height for the two regions reaches 714 m and 794 m at 120 m/s with a typical return stroke peak current of 30 kA respectively, there is about 11.2% difference between the two regions. It can be inferred that the region where the blade pressure is higher will face more risk of lightning strikes than the lower-pressure region. The lightning protection device is recommended to be installed at the high pressure area of the blade.
3 The attack angle has a more significant impact than velocity on the positive streamer gradient, and the tends to increase gradually as the attack angle increases. It is noteworthy that the difference has reached about 28% for the attack angle of 10°. According to the simulated results, it can be concluded that the probability of lightning strikes in the low-pressure area of the blade will be reduced as the attack angle increases.

When the downward stepped leader is descending to a certain height, the upward leader will be initiated at the areas where the conditions are satisfied. After the height of the developing stepped leader decreases further, other places will also meet the conditions of the upward leader initiation. Therefore, more than one upward leader could be generated in the process of the downward stepped leader development. In general, the upward leader that initiates in the first place gets more time to develop an extended channel and has a higher probability of eventually connecting with the downward stepped leader to discharge. Nevertheless, according to the observation data, although the upward leader is successfully initiated and developed subsequently, there are still cases where the initiation point fails to become a lightning strike point. However, in this paper, it is still considered that the successful initiation of the upward leader is an important indication of the lightning strike, ignoring the development process after the initiation.

Data Availability statement

The raw data supporting the conclusion of this article will be made available by the authors, without undue reservation.

Author contributions

NY and WH, contributed to conception and design of the study. WJ and CJ organized the database. NY performed the analysis. NY wrote the first draft of the manuscript. SZ verify the manuscript. All authors contributed to manuscript revision, read, and approved the submitted version.

Funding

This work is supported by Natural Science Foundation of Jiangsu Province (Grants No: BK20200175); Major Basic Research Project of Natural Science Foundation of Jiangsu Higher Education (1KJA460001).

Conflict of interest

The authors declare that the research was conducted in the absence of any commercial or financial relationships that could be construed as a potential conflict of interest.

Publisher's note

All claims expressed in this article are solely those of the authors and do not necessarily represent those of their affiliated organizations, or those of the publisher, the editors and the reviewers. Any product that may be evaluated in this article, or claim that may be made by its manufacturer, is not guaranteed or endorsed by the publisher.

References

Agoris, D. (2002). "Analysis of lightning incidents on wind turbines in Greece," in Proceedings of the 26th International Conference on Lightning Protection (ICLP 2002), Cracow, Poland, 2nd - 6th September 2002, 717–721.

Becerra, M., and Cooray, V. (2006a). A self-consistent upward leader propagation model. *J. Phys. D Appl. Phys.* 39 (16), 3708–3715. doi:10.1088/0022-3727/39/16/028

Becerra, M., and Cooray, V. (2006b). A simplified physical model to determine the lightning upward connecting leader inception. *IEEE Trans. Power Deliv.* 21 (2), 897–908. doi:10.1109/tpwrd.2005.859290

Beckers, R. (2016). Lightning protection. Available at: http://www.solacity.com/lightning-protection/.

Comsol Group (2014). *User's guide*. Stockholm, Sweden: Comsol Group.

Cooray, V., Rakov, V., and Theethayi, N. (2007). The lightning striking distance—Revisited. *J. Electrost.* 65 (5-6), 296–306. doi:10.1016/j.elstat.2006.09.008

Cotton, I., Jenkins, N., and Pandiaraj, K. (2001). Lightning protection for wind turbine blades and bearings. *Wind Energy Int. J. Prog. Appl. Wind Power Convers. Technol.* 4 (1), 23–37. doi:10.1002/we.44

Eriksson, A. J., Le Roux, B. C., Geldenhuys, H. J., and Meal, D. V. (1986). Study of airgap breakdown characteristics under ambient conditions of reduced air density. *IEE Proc. A Phys. Sci. Meas. Instrum. Manag. Educ. Rev.* 133 (8), 485–492. doi:10.1049/ip-a-1.1986.0067

Gallimberti, I. (1979). The mechanism of the long spark formation. *Le J. de Physique Colloques* 40 (C7), C7. doi:10.1051/jphyscol:19797440

Garolera, A. C., Madsen, S. F., Nissim, M., Myers, J. D., and Holboell, J. (2014). Lightning damage to wind turbine blades from wind farms in the US. *IEEE Trans. Power Deliv.* 31 (3), 1043–1049. doi:10.1109/tpwrd.2014.2370682

Gcube-insurance (2012). GCube top 5 US wind energy insurance claims report. Available at: http://www.gcube-insurance.com/en/press/gcube-top-5-us-wind-energy-insurance-claims-report/.

Global Wind Energy Council (2022). *Global wind report 2022*. Belgium: GWEC.

Goelian, N., Lalande, P., Bondiou-Clergerie, A., Bacchiega, G. L., Gazzani, A., and Gallimberti, I. (1997). A simplified model for the simulation of positive-spark development in long air gaps. *J. Phys. D Appl. Phys.* 30 (17), 2441–2452. doi:10.1088/0022-3727/30/17/010

Gu, J., Huang, S., Fu, Y., Chen, W., Cheng, D., Shi, W., et al. (2020). Morphological characteristics of streamer region for long air gap positive discharge. *J. Phys. D Appl. Phys.* 54 (2), 025205. doi:10.1088/1361-6463/abbeb3

Hu, Q., Shu, L., Jiang, X., Sun, C., Zhang, S., and Shang, Y. (2011). Effects of air pressure and humidity on the corona onset voltage of bundle conductors. *IET generation, Transm. distribution* 5 (6), 621–629. doi:10.1049/iet-gtd.2010.0560

Lalande, P., Bondiou-Clergerie, A., Bacchiega, G., and Gallimberti, I. (2002). Observations and modeling of lightning leaders. *Comptes Rendus Phys.* 3 (10), 1375–1392. doi:10.1016/s1631-0705(02)01413-5

Madsen, S. F., Holbøll, J., Henriksen, M., and Sørensen, T. (2006). "Interaction between electrical discharges and materials for wind turbine blades particularly related to lightning protection," in *Ørsted–DTU, electric power engineering* (Lyngby, Denmark: Technical University of Denmark). PhD thesis.

Qu, L., Wang, Y., Liu, G., Liao, M., Cai, H., Zhang, T., et al. (2019). Simulation study on positive corona discharge of receptors on rotating wind turbine blade tips under thundercloud electric fields. *Energies* 12 (24), 4696. doi:10.3390/en12244696

Rademakers, L. W., Braam, H., Ramakers, S. G., Wessels, H. R., Prins, R. K., Lok, R., et al. (2002). Netherlands: Energy research Centre of the Netherlands.Lightning damage of OWECS. Part 1.'Parameters relevant for cost modelling

Radičević, B. M., Savić, M. S., Madsen, S. F., and Badea, I. (2012). Impact of wind turbine blade rotation on the lightning strike incidence–A theoretical and experimental study using a reduced-size model. *Energy* 45 (1), 644–654. doi:10.1016/j.energy.2012.07.032

Ramirez, M., Moreno, M., Pigini, A., Rizzi, G., and Garbagnati, E. (1990). Air density influence on the strength of external insulation under positive impulses: Experimental investigation up to an altitude of 3000 m asl. *IEEE Trans. power Deliv.* 5 (2), 730–737. doi:10.1109/61.53076

Sorensen, T. (1998). *Lightning damages to power generating wind turbines*. Birmingham, UK: ICLP-98.

Wen, X., Qu, L., Wang, Y., Chen, X., Lan, L., Si, T., et al. (2016). Effect of wind turbine blade rotation on triggering lightning: An experimental study. *Energies* 9 (12), 1029. doi:10.3390/en9121029

Yang, N., Zhang, Q., Hou, W., and Wen, Y. (2017). Analysis of the lightning attractive radius for wind turbines considering the developing process of positive attachment leader. *J. Geophys. Res. Atmos.* 122, 3481–3491. doi:10.1002/2016JD026073

Yu, D., Farzaneh, M., Zhang, J., Shu, L., Sima, W., and Sun, C. (2006). "Properties of corona discharge under positive DC voltage at low atmospheric pressure," in Proceedings of the 2006 IEEE Conference on Electrical Insulation and Dielectric Phenomena, Denver, CO, USA, 15-18 Oct. 2006 (IEEE), 393–396.

Yu, W. A. N. G., Lu, Q. U., Tianjun, S. I., Yang, N. I., Jianwei, X. U., and Xishan, W. E. N. (2017). Experimental study of rotating wind turbine breakdown characteristics in large scale air gaps. *Plasma Sci. Technol.* 19 (6), 064016. doi:10.1088/2058-6272/aa6743

Yu, W., Li, Q., Zhao, J., and Siew, W. H. (2022). Numerical simulation of the lightning leader development and upward leader initiation for rotating wind turbine. *Machines* 10 (2), 115. doi:10.3390/machines10020115